Check for updates

Received: 24 August 2020 | Revised: 17 February 2021 | Accepted: 23 February 2021

DOI: 10.1111/pce.14039

ORIGINAL ARTICLE

Plant, Cell & Environment WILEY

Proteomic analysis reveals how pairing of a Mycorrhizal fungus with plant growth-promoting bacteria modulates growth and defense in wheat

Candida Vannini[1] | Guido Domingo[1] | Valentina Fiorilli[2] | Daniel Garçia Seco[3] | Mara Novero[2] | Milena Marsoni[1] | Florence Wisniewski-Dye[4] | Marcella Bracale[1] | Lionel Moulin[3] | Paola Bonfante[2]

[1]Dipartimento di Biotecnologie e Scienze della Vita, Università degli Studi dell'Insubria, Varese, Italy

[2]Department of Life Sciences and Systems Biology, Università degli Studi di Torino, Torino, Italy

[3]IRD, CIRAD, University of Montpellier, IPME, Montpellier, France

[4]Univ Lyon, Université Claude Bernard Lyon 1, CNRS, INRAE, VetAgroSup, UMR Ecologie Microbienne, Villeurbanne, France

Correspondence
Candida Vannini, Dipartimento di Biotecnologie e Scienze della Vita, Università degli Studi dell'Insubria, via J.H Dunant 3, 21100, Varese, Italy.
Email: candida.vannini@uninsubria.it

Funding information
Agropolis Fondation, Grant/Award Number: Project ID 1301-003; Fondazione Cariplo, Grant/Award Number: Project ID 2013-1888

Abstract

Plants rely on their microbiota for improving the nutritional status and environmental stress tolerance. Previous studies mainly focused on bipartite interactions (a plant challenged by a single microbe), while plant responses to multiple microbes have received limited attention. Here, we investigated local and systemic changes induced in wheat by two plant growth-promoting bacteria (PGPB), *Azospirillum brasilense* and *Paraburkholderia graminis*, either alone or together with an arbuscular mycorrhizal fungus (AMF). We conducted phenotypic, proteomic, and biochemical analyses to investigate bipartite (wheat–PGPB) and tripartite (wheat–PGPB–AMF) interactions, also upon a leaf pathogen infection. Results revealed that only AMF and *A. brasilense* promoted plant growth by activating photosynthesis and N assimilation which led to increased glucose and amino acid content. The bioprotective effect of the PGPB–AMF interactions on infected wheat plants depended on the PGPB-AMF combinations, which caused specific phenotypic and proteomic responses (elicitation of defense related proteins, immune response and jasmonic acid biosynthesis). In the whole, wheat responses strongly depended on the inoculum composition (single vs. multiple microbes) and the investigated organs (roots vs. leaf). Our findings showed that AMF is the best-performing microbe, suggesting its presence as the crucial one for synthetic microbial community development.

KEYWORDS
Azospirillum brasilense, bi- and tripartite interaction, *Funneliformis mosseae*, growth and defense response, *Paraburkholderia graminis*, pathogens, proteome, *Xanthomonas translucens*

1 | INTRODUCTION

Like humans, animals and fungi, plants live among a variety of microbial species, which together comprise the plant microbiota (Schlaeppi & Bulgarelli, 2015). Plant root-associated microbes have received increasing attention, starting from their taxonomic description (Bulgarelli et al., 2012; Lundberg et al., 2012) to their role in plant health (Müller, Vogel, Bai, & Vorholt, 2016). Data generated by multiple omics approaches demonstrate that the plant microbiota does not represent a random assembly of microbes living in the soil. On the contrary, plant microbiota composition is determined by an active host plant-driven selection process, which depends on the plant genotype, environmental conditions and microbial interactions (Durán et al., 2018; Hacquard et al., 2015; Saad, Eida, & Hirt, 2020; Thiergart

Candida Vannini, Guido Domingo and Valentina Fiorilli contributed equally to this work.

 © 2021 John Wiley & Sons Ltd.

et al., 2019; Uroz, Courty, & Oger, 2019). The complexity of the microbial community structure parallels the many beneficial functions currently assigned to the plant microbiota: stimulation of plant growth through phytohormone production, improvement of the plant nutrient status through the increased uptake of nutrients such as inorganic phosphate (Pi) and nitrogen (N) and increased availability of nutrients such as iron, greater tolerance to abiotic stress (e.g., drought) and biotic stress, and increased activation of plant innate immunity (Hacquard, Spaepen, Garrido-Oter, & Schulze-Lefert, 2017). Many of these benefits have been traditionally associated with the so-called plant growth-promoting bacteria (PGPB), as well as with the root symbionts, such as arbuscular mycorrhizal (AM) fungi and N-fixing bacteria (Lugtenberg, Caradus, & Johnson, 2016). Comparison of the data generated by culture-independent approaches with the knowledge obtained from the investigation of controlled binary interactions of bacterial and fungal isolates with their host plant has led to the creation of the so-called synthetic communities (SynComs) (Herrera Paredes et al., 2018; Tsolakidou et al., 2019). Simultaneous inoculation of the host plant with several different beneficial microbes allows the investigation of plant responses under controlled and reproducible conditions. These new tools therefore form the basis of the so-called microbial revolution, defined as the microbe-driven increase in crop productivity, leading to higher sustainability (Baez-Rogelio, Morales-García, Quintero-Hernández, & Muñoz-Rojas, 2017).

Together with rice and corn, wheat is one of the most important crops worldwide (Fernie & Yan, 2019). Recently, many studies have been conducted on wheat-associated microbes, providing a detailed list of bacteria and fungi associated with wheat plants under natural conditions (Kuźniar et al., 2020; Mahoney, Yin, & Hulbert, 2017; Naylor, DeGraaf, Purdom, & Coleman-Derr, 2017; Pagé, Tremblay, Masson, & Greer, 2019) or describing the core microbiome of wheat (Simonin et al., 2020), thus revealing the ecological rules that regulate microbial assembly (Hassani, Özkurt, Seybold, Dagan, & Stukenbrock, 2019). Ecological studies suggest that higher soil microbial diversity results in a greater resilience of the plant population (Van der Heijden et al., 1998). However, the assumption that a mixture of beneficial microbes automatically provides greater plant protection is an oversimplification (Rosier, Bishnoi, Lakshmanan, Sherrier, & Bais, 2016). In this context, the responses of wheat to its microbiota are still unknown.

In this study, to disentangle the inherent complexity of plant–microbiota interactions (Vorholt, Vogel, Carlström, & Müller, 2017), we followed a reductionist approach, where we selected two PGPB species, *Azospirillum brasilense* and *Paraburkholderia graminis*, which are associated with wheat plants under natural conditions, as well as an arbuscular mycorrhizal fungus (AMF), *Funneliformis mosseae*. We hypothesized that targeted inoculation of wheat plants with the AMF and one of the two PGPB could provide an experimentally tractable system for evaluating the outcome of the interaction between beneficial microbes. Previously, we demonstrated that inoculation with *F. mosseae* improved plant growth and enhanced bioprotection in wheat (Fiorilli et al., 2018). The current study aimed to investigate the long-term local and systemic effects of *P. graminis* or *A. brasilense* on the wheat proteome in non-mycorrhizal and mycorrhizal plants. We compared the proteomic changes in wheat triggered by co-inoculation of PGPB and *F. mosseae* with those elicited by single inoculations. In addition, we investigated the bioprotective effects of bipartite (wheat–PGPB) and tripartite (wheat–PGPB–AMF) interactions on wheat plants against the leaf pathogen, *Xanthomonas translucens*. While *A. brasilense* drastically altered the bioprotective effect of the AMF, *P. graminis* did not affect AMF-induced pathogen resistance. Overall, proteomic changes revealed the molecular mechanisms underlying the tripartite interaction and showed that the beneficial effects of the AMF on plants are differentially modulated by the plant-associated PGPB.

2 | MATERIALS AND METHODS

2.1 | Bacterial strains, mycorrhizal fungus and wheat genotype

Two plant growth promoting bacteria (PGPB), *Azospirillum brasilense* Sp245 (obtained from UMR Ecologie Microbienne, Villeurbanne) and *Paraburkolderia graminis* C4D1M (type strain of the species, LMG collection, Ghent, Belgium), one wheat pathogen, *Xanthomonas translucens* CFBP2054 (obtained from CFBP collection), and one mycorrhizal fungus, *Funneliformis mosseae* (BEG.12, MycAgro Lab, France) were used in our experiments.

In detail, *A. brasilense* strain Sp245 was isolated from wheat roots and was shown to stimulate root development and increase plant dry mass (Kapulnik, Okon, & Henis, 1985), while the strain C4D1M of *P. graminis* was isolated from senescent corn roots and found to positively interact with different species of wheat (Moulin, personal communication).

Gfp-tagged derivatives were also included for cytology analyses: *A. brasilense* Sp245 eGFP carrying the pMP2444 plasmid eGFP, GmR (Wisniewski-Dyé et al., 2011) and *P. graminis* C4D1M eGFP, constructed by triparental mating (using a Tn7 eGFP construct described in [Norris, Kang, Wilcox, & Hoang, 2010] with a single insertion of the Tn7 upstream of the *glmS* gene). *A. brasilense* was cultivated at 28°C on LBA medium (Luria Broth low salt, agar) and *P. graminis* in YMA medium (yeast extract, 3 g; mannitol, 10 g; KH_2PO_4, 0.5 g; $MgSO_4$, 0.2 g; NaCl, 0.1 g; agar, 18 g; distilled water, 1 L; pH 6.8) and grown overnight in the same broth medium for inoculation. Strains were stored at −80°C in 20% glycerol. *X. translucens* CFBP 2054 was grown at 28°C on Peptone sucrose agar (PSA) medium, retrieved from Petri dish with sterile water to reach OD 0.5 for leaf clipping and infiltration assays.

The *Triticum aestivum* cv Chinese Spring was used for all experiments (seeds obtained from Valeria Terzi, CREA, Italy).

2.2 | Plant material and plant inoculations

The methodologies have already been described in previous articles on the wheat response to *Xanthomonas* (Garcia-Seco et al., 2017) and to mycorrhizal fungi (Fiorilli et al., 2018). Twelve combinations were studied: (1) control plants (C), (2) *A. brasilense*-inoculated plants (Az), (3) *P. graminis*-inoculated plants (P), (4) *F. mosseae*-inoculated plants

(M), (5) C + *Xanthomonas translucens* (X), (6) Az + X, (7) P + X, (8) M + X, (9) Az + M, (10) P + M, (11) Az + M + X, (12) P + M + X. An overview of the experiment is given in Figure S1.

Seeds were disinfected by immersing for 40 minutes in a sodium hypochlorite solution and washed with sodium thiosulfate and pregerminated. The seedlings were transferred to pots containing a mix of sterile quartz sand + either the *F. mosseae* carrier inoculum substrate (the substrate without the fungus) for control and PGPB conditions, or the *F. mosseae* inoculum (30% v/v) for mycorrhizal and mycorrhizal + PGPB conditions. PGPB were inoculated directly after seedling transfer to pots, with 1 mL per plant at OD 1 from an overnight broth culture washed once and diluted with water.

For each inoculated condition, 10 pots containing 1 plant were used for phenotyping of root and fresh weight at 50 dpi, 5 pots were used for proteomic, and 5 pots for leaf-clipping assays with *Xanthomonas translucens*.

All plants were maintained under glasshouse conditions under cycles of 12 hours of light at 21°C and 50% relative humidity (RH) and 12 hours of dark at 21°C and 50% RH, watered twice a week with water, and once with a modified Long-Ashton solution containing a low phosphorous concentration (32 μM Na_2HPO_4*$12H_2O$).

Spikes weight were measured separately in the mature plants at the end of their natural cycle. The spikes were threshed and 1,000-kernel weights were determined.

For *Xanthomonas* infections, two types of inoculation were performed. A phenotyping leaf-clipping assay with scissors soaked in a 0.5 OD *X. translucens* culture was performed at 46 dpi on a first set of plants for phenotyping the length of the symptoms at 4-day post-clipping (dpc; starting point of the lesions) and 26 dpc. A second set of plants dedicated to proteomic analyses was infiltrated at 49 dpi with a 0.5 OD *X. translucens* culture using a microneedle, as described in Garcia-Seco et al. (2017), and sampled the following day.

2.3 | Evaluation of wheat roots microbial colonization

The mycorrhizal and mycorrhizal + PGPB roots were stained with 0.1% cotton blue and the level of mycorrhizal colonization was assessed as previously described (Trouvelot, Kough, & Gianinazzi-Pearson, 1986).

For Colony Forming Unit (CFU) counting from plant roots, root fragments were weighted then pulverized with a FastPrep™ in tubes containing a ceramic bead in 500 μL of sterile water, centrifuged at 1000 rpm for 30 seconds and drops of 20 μL of serial dilutions were plated on bacterial media and counted 24 hours later.

2.4 | Proteomic analysis and data processing

Plant samples (root and leaves) were sampled at 50 dpi and pulverized with liquid nitrogen. The used protocol for total protein extraction was based on SDS and phenol extraction (Wu, Xiong, Wang, Scali, & Cresti, 2014). Then, samples were digested and analysed by Liquid Chromatography-Mass Spectrometry (LC-MS/MS) as described previously (Garcia-Seco et al., 2017). Mass spectrometer raw files were analysed by MaxQuant (version 1.6.2.3, default parameters) against UniProt *T. aestivum* (Version 2017-1, 150,716 entries), Uniprot *Rhizophagus irregularis* (Version 2015-10, 29,847 entries), Uniprot *P. graminis* (Version 2015-10, 6,732 entries) and Uniprot *A. brasilense* (Version 2015-10, 7,636 entries). On January 2019, the UniProt *T. aestivum* database has been updated. Therefore, we obtained the updated protein IDs by BLAST search of our dataset against the Uniprot *T. aestivum* 2019 database (143,020 entries). Unknown proteins were annotated by BLAST search against the Uniprot viridiplantae database (Version 2019-01, 6,913,939 entries), taking the first hit with a valid annotation.

All MS proteomic data have been deposited in the ProteomeXchange Consortium via PRIDE partner repository with the Username: reviewer04430@ebi.ac.uk and Password: 2vlyEEVZ.

MaxQuant output files were processed as described earlier (Vannini et al., 2019). Only proteins detected in at least two of the three biological replicates (75%) sharing the same treatment and tissue were considered.

To compare the differences among analytical groups we performed an ANOVA based multiple samples coupled with Tukey test using the *R* package LIMMA. Only proteins with false discovery rate (FDR) below 0.01 were considered differentially abundant proteins (DAPs) within the various comparisons. In order to produce a reliable and robust dataset, all proteins which gave one nonzero and two zero outcomes (two-time imputation) in at least one of the samples in each comparison were considered unreliable and therefore eliminated.

In order to use bioinformatic tools available only for *A. thaliana*, a local BLAST of *T. aestivum* proteins against the TAIR10 database (version May 7, 2012) was performed.

The enrichment analysis was performed using the Gene Ontology Resource (http://geneontology.org), running PANTHER algorithm with *A. thaliana* as background and FDR < 0.05 or using the AgriGO Singular Enrichment Analysis (SEA) compare tool (http://bioinfo.cau.edu.cn/agriGO/analysis.php?method=compare), with *A. thaliana* TAIR10_2017 protein database as background, default parameters and a FDR threshold of 0.05 (Du, Zhou, Ling, Zhang, & Su, 2010).

2.5 | Amino acid analysis

For the amino acids (AAs) extraction, 0.1 g of lyophilized samples were re-suspended in 10 mL of 0.1% (v/v) formic acid in water/methanol (50:50). 10 μL of 10 mM deuterated internal standards (L-Phenyl-d5-alanine and L-alanine ^{15}N Met) were added. Free AAs were quantified by liquid chromatography tandem mass spectrometry (LC-MS/MS) as described previously (Fiorilli et al., 2018).

2.6 | Total glucose and nitrogen content

Soluble sugars were extracted as described by (Shi, Wang, Yang, Li, & Miao, 2016) with minor modifications. Briefly, 0.2 g of leaves material

were boiled (80°C) in ethanol 80% for 30 minutes. After centrifugation (13,000*g* × 5 minutes) the supernatant was recovered. The extraction was repeated twice and all supernatants were collected. Sucrose in solution was hydrolysed with HCl (2% of HCl concentrated V/V) for 5 minutes at 90°C. After acid neutralization by KOH (5% of 5 N KOH V/V) total glucose was estimated by the dinitrosalicylic (DNS) method (Miller, 1959).

Wheat root N content was determined by CHNS elemental analyzer Thermo Fisher Scientific following the manufacturer's specifications. About 2–3 mg of sample for each replicate were weighed and placed in a tin capsule containing 9.5 to 10.5 mg of vanadium pentoxide. The N_2 product by sample combustion was quantitatively determined through a separation with a gas chromatograph (GC) followed by a quantification using a thermal conductivity detector. Three tests were prepared for each sample.

2.7 | Statistics

Phenotyping data of plant weight, CFU and lesion length were analyzed, depending on normality of data, by ANOVA followed by Tukey post-hoc test or Kruskal–Wallis test followed by Mann–Whitney pairwise comparisons, in R Environment (rstatix) and figures produced by ggplot.

Data from quantification of amino acid, total glucose and nitrogen were subjected to statistical analysis by ANOVA and Tukey post-hoc test.

3 | RESULTS

3.1 | PGPB and AMF impact plant growth

Wheat plants were inoculated with *A. brasilense* Sp245, *P. graminis* C4D1M, *A. brasilense* Sp245 plus *F. mosseae*, or *P. graminis* C4D1M plus *F. mosseae* (hereafter referred to as Az, P, AzM and PM plants, respectively) and grown under controlled conditions (Figure S1). The root and shoot biomass of these plants was determined at 50 days post-inoculation (dpi) and compared with that of mock-inoculated control (C) and *F. mosseae* only-inoculated (M) plants. In isolation, *A. brasilense* Sp245 exerted a strong positive effect on the growth of roots and shoots, whereas *P. graminis* C4D1M did not induce statistically significant growth of these organs (Figure 1). Monitoring these plants until seed production revealed that *P. graminis* significantly increased the seed yield, doubling the spike weight (Figure S2).

To determine whether the positive impact of the two PGPB on plant growth was associated with an efficient colonization process, bacteria on the root surface were counted at different time points. *A. brasilense* exhibited the greatest colonizing potential, with the bacterial count remaining constant across different time points. Colonization by *P. graminis* decreased with time to 1×10^2 colony forming units (CFU) at 21 dpi (Figure S3). The success of AMF colonization was evaluated at 50 dpi by calculating the total length of colonized roots (F%) and total number of arbuscules (A%) in plants inoculated with AMF alone or AMF plus PGPB (*A. brasilense* or *P. graminis*). Colonization by the AMF resulted in abundant arbuscules in all plants. No

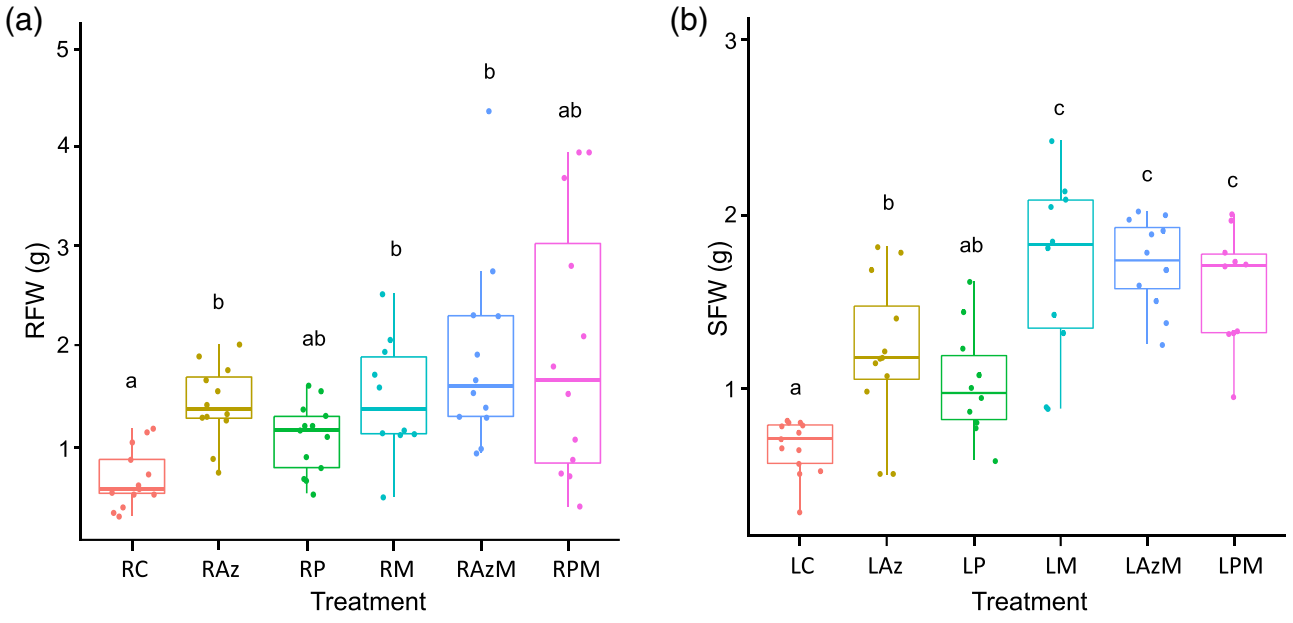

FIGURE 1 Effect of arbuscular mycorrhizal (AM) symbiosis on the biomass of different organs of wheat plants. (a) Fresh weight of roots (RFW; grams). (b) Fresh weight of shoots (SFW; grams). Plants were either mock-inoculated (control; C) or inoculated with different microbial combinations: *Azospirillum brasilense* only (Az), *Paraburkholderia graminis* only (P), *Funneliformis mosseae* only (M), *A. brasilense* plus *F. mosseae* (AzM), and *P. graminis* plus *F. mosseae* (PM). Wheat plants were harvested at 50 days post-inoculation (dpi). Data represented as mean ± standard deviation (SD; $n \geq 6$) were subjected to a one-way analysis of variance (ANOVA). Different lowercase letters indicate significant differences ($p < .05$; Tukey's test) [Colour figure can be viewed at wileyonlinelibrary.com]

differences were detected in F% and A% among plants inoculated with AMF alone or together with PGPB, indicating that the presence or absence of PGPB does not affect mycorrhizal colonization (Figure S3).

The shoot weight of AzM and PM plants was significantly higher than that of Az and P plants (Figure 1b) but comparable with that of M plants, indicating that PGPB did not lead to any additional yield benefit compared with the mycorrhizal condition.

3.2 | AMF alone or in combination with a PGPB triggers different responses to *X. translucens* infection

Inoculated wheat plants were assessed for protective effect to *X. translucens* leaf infection by leaf-clipping plants with the pathogen at 46 dpi and recording leaf symptoms at 4 and 26 days post-leaf clipping (dpc). Pathogen-infected plants were identified as AzX, PX, MX, AzMX and PMX and positive control plants as CX. Disease symptoms were evident in CX plants at 4 and 26 dpc (Figure 2). Lesion length in MX plants was significantly less than that in CX plants both at 4 and 26 dpc, consistent with our previous results (Fiorilli et al., 2018).

Lesion length appeared extended in AzX and CX plants at both time points. AzMX plants showed reduced symptoms in comparison with AzX plants at 4 dpc but showed extended lesions compared with CX and AzX plants at 26 dpc. This result indicates that the *F. mosseae*-induced bioprotection in wheat is abrogated between 4 and 26 dpc in the presence of *A. brasilense*.

At 26 dpc, a significant reduction in symptoms was observed only in MX and PMX plants when compared with CX plants, whereas lesions were significantly increased in AzX and AzMX plants compared with PX, MX and PMX plants. These results indicate that inoculation with *F. mosseae* alone (Fiorilli et al., 2018) or in combination with *P. graminis* increased protection against *X. translucens*. Overall, this experiment showed that *A. brasilense* inoculation alone did not protect wheat plants against the pathogen, and rather undermined the positive effect exerted by *F. mosseae*.

3.3 | Quantitative overview of proteomics analysis

We conducted proteomic analysis of the roots (R) of Az, P, M, AzM and PM plants (hereafter referred to as RAz, RP, RM, RAzM and RPM samples, respectively) as well as the leaves of these plants (hereafter referred to as LAz, LP, LM, LAzM and LPM samples, respectively). In addition, we performed proteomic analysis of the leaves of these plants following infection with *X. translucens* (hereafter referred to as LAzX, LPX, LMX, LAzMX and LPMX, respectively). Each treatment was analyzed in triplicate.

A total of 3,846 and 3,883 wheat proteins were identified and quantified in root and leaf samples, respectively. Samples were clustered by condition according to their protein expression patterns (Figure S4). Replicates within each analytical group clustered together, confirming the high reproducibility of biological replicates. Protein abundance was compared between samples, and differentially abundant proteins (DAPs) were identified using the following thresholds:

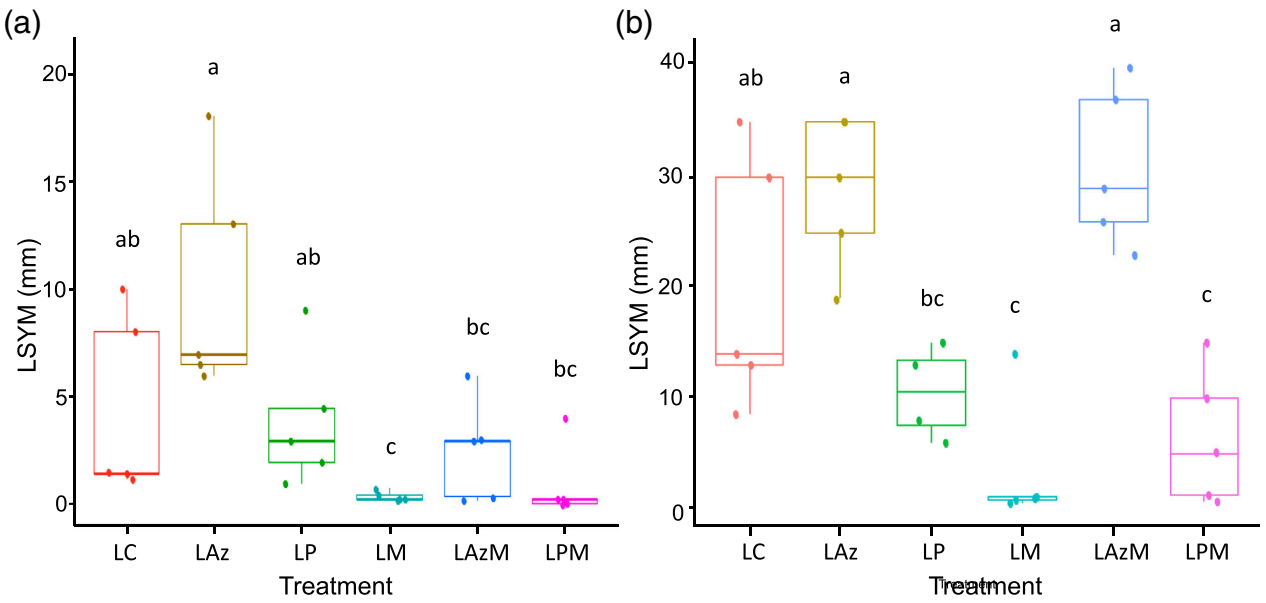

FIGURE 2 Phenotypic evaluation of disease symptoms caused by the bacterial pathogen *Xanthomonas translucens*. Lesion length (mm) was assessed on leaves of C, Az, P, M, AzM and PM plants at 4 (a) and 26 (b) days post-leaf clipping (dpc). Data at 4 dpc (not normally distributed) were analysed using the Kruskal-Wallis test. Asterisks indicate significant differences at the 5% level using Mann–Whitney pairwise comparisons. Data at 26 dpc were subjected to one-way analysis of variance (ANOVA). Different lowercase letters indicate significant differences ($p < .05$; Tukey's test) [Colour figure can be viewed at wileyonlinelibrary.com]

false discovery rate (FDR) < 0.01 and log_2fold-change (log_2FC) > 0.5 (Tables S1–S5 and S7–S15).

Functional characterization of DAPs was conducted with Gene Ontology (GO) enrichment analysis to determine the main biological processes stimulated by microbial inoculations.

In root samples, approximately 7%, 0.6% and 0.6% of all identified proteins were assigned to AMF, *A. brasilense* and *P. graminis* proteomes, respectively, confirming the presence of all three root-associated microbes at harvest.

3.4 | Wheat response to single inoculation: An overview

A large number of significant DAPs (p < .01) were identified; 639 DAPs (386 in leaves and 253 in roots) in the C versus Az comparison, and 1,085 DAPs (424 in leaves and 661 in roots) in the C versus P comparison (Tables S1–S4). In leaves, approximately 50% of the DAPs were common between the C versus Az and C versus P comparisons (Figure S5a). By contrast, in roots, proteomic expression was highly specific, mirroring the stronger impact on the colonized niche; only 12% of the DAPs were common between the C versus Az and C versus P comparisons (Figure S5b).

To decipher the molecular mechanisms involved in *A. brasilense*-induced plant growth promotion, we performed GO enrichment analysis of LAz versus LC, LP versus LC, Raz versus RC and RP versus RC (Figure 3). In leaf samples, 'photosynthesis light harvesting' and 'photosynthetic electron transport chain' were the two most enriched GO terms. These data were consistent with the higher total glucose content of LAz samples compared with LC, LP and LM samples (Figure 4a). Our experiments, therefore, confirmed that *A. brasilense* exhibits a greater ability to drive an increase in the glucose content of

GO biological process complete	Fold Enrichment
RAz vs RC	
isopentenyl diphosphate biosynthetic process	40.48
aldehyde catabolic process	35.98
hydrogen peroxide metabolic process	29.98
phenylpropanoid biosynthetic process	12.27
response to wounding	7
response to cadmium ion	5.48
monocarboxylic acid metabolic process	4.92
response to oxidative stress	4.74
plant-type primary cell wall biogenesis	43.84
cellulose biosynthetic process	34.1
cell cycle	7.12
carboxylic acid biosynthetic process	6.06
RP vs RC	
glyceraldehyde-3-phosphate metabolic process	50.3
gluconeogenesis	27.34
long-chain fatty acid metabolic process	26.95
isopentenyl diphosphate metabolic process	23.58
malate metabolic process	20.96
lignin biosynthetic process	20.96
jasmonic acid biosynthetic process	19.35
defense response to fungus	15.4
glycolytic process	13.97
tricarboxylic acid cycle	13.67
cellular detoxification	12.9
reactive oxygen species metabolic process	10.94
response to cadmium ion	9.18
cellular amino acid biosynthetic process	4.88
root morphogenesis	4.24
response to bacterium	3.73
pre-replicative complex assembly	37.9
response to desiccation	18.42
fatty acid beta-oxidation	11.95
tRNA aminoacylation for protein translation	9.15
lignin metabolic process	8.34
response to cadmium ion	5.05
ATP metabolic process	4.88

GO biological process complete	Fold Enrichment
LAz vs LC	
coumarin biosynthetic process	67.67
photosynthesis, light harvesting in photosystem II	60.92
photosynthetic electron transport chain	26.49
lignin biosynthetic process	24.18
purine ribonucleoside triphosphate biosynthetic process	16.25
response to toxic substance	8.46
cellular amino acid biosynthetic process	5.91
translation	3.97
protein targeting to chloroplast	16.02
cellular biogenic amine biosynthetic process	13.4
porphyrin-containing compound biosynthetic process	12.28
protein folding	9.88
aromatic amino acid family metabolic process	8.37
response to cadmium ion	4.68
response to bacterium	3.5
LP vs LC	
S-adenosylmethionine biosynthetic process	97.91
lignin biosynthetic process	27.98
tetrahydrofolate metabolic process	26.11
glucose metabolic process	18.65
response to cadmium ion	13.06
response to toxic substance	8.16
generation of precursor metabolites and energy	5.71
purine ribonucleotide metabolic process	5.90
oxidation-reduction process	4.09
L-phenylalanine catabolic process	32.48
malate metabolic process	21.66
protein targeting to chloroplast	14.12
cellular biogenic amine biosynthetic process	11.81
indole-containing compound biosynthetic process	10.39
cell redox homeostasis	9.02
response to cadmium ion	5.36
protein folding	5.08
nucleotide metabolic process	4.62
translation	4.32

FIGURE 3 Gene ontology (GO) enrichment analysis of DAPs identified by comparing Az or P versus C roots (RAz vs. RC and RP vs. PC) and leaves (LAz vs. LC and LP vs. LC). Enriched GO terms were selected using the following thresholds: false discovery rate (FDR) ≤ 0.05 and fold enrichment >3.5. Red and blue indicate the enrichment of GO biological process terms for up-and down- regulated DAPs, respectively [Colour figure can be viewed at wileyonlinelibrary.com]

shoots than other beneficial microorganisms (*F. mosseae* and *P. graminis*). Moreover, the LAz sample showed a higher abundance of sucrose transporter 2D (SUT2D) than the LC sample; SUT2D shows high similarity to rice SUT2 (OsSUT2), which is involved in sucrose mobilization to sink cells (Eom et al., 2011).

The 'amino acid metabolism' GO term was highly enriched in enzymes involved in the synthesis of aspartate, proline and branched-chain amino acids. The increased content of amino acids both in root and leaf samples validated the proteomics data (Table S6). The presence of *A. brasilense* on wheat roots also increased the abundance of the phosphate transporter Pht1-10, which is induced by the AMF (Fiorilli et al., 2018) and enhances Pi uptake. Interestingly, the abundance of Pht1-10 was lower in the RP sample versus RC (Figure S6). Moreover, Pht1-10 was among the four proteins whose abundance showed opposite trends between RAz and RP samples (Table S5). Plants assimilate and metabolize ammonium (NH_4^+) provided by diazotrophs, including *Azospirillum* spp. (Carvalho, Balsemão-Pires, Saraiva, Ferreira, & Hemerly, 2014). In LAz samples, we observed an increase in the abundance of ferredoxin-glutamate dehydrogenase, 2-oxoglutarate (2-OxG)/malate translocator, and isocitrate dehydrogenase (ICDH), and a decrease in the abundance of ferredoxin-nitrite reductase; both these trends are indicative of a higher NH_4^+ assimilation rate in the leaves of Az plants. The increase in photosynthesis could contribute to enhanced tolerance to NH_4^+ toxicity by increasing NH_4^+ assimilation (Setién et al., 2013). Higher concentrations of free amino acids and N in RAz samples support these proteomic results (Table S6 and Figure 4b).

In roots and leaves, inoculation with *A. brasilense* stimulated the mitochondrial electron transport for ATP synthesis, even if the proteins involved were different (Tables S1 and S2).

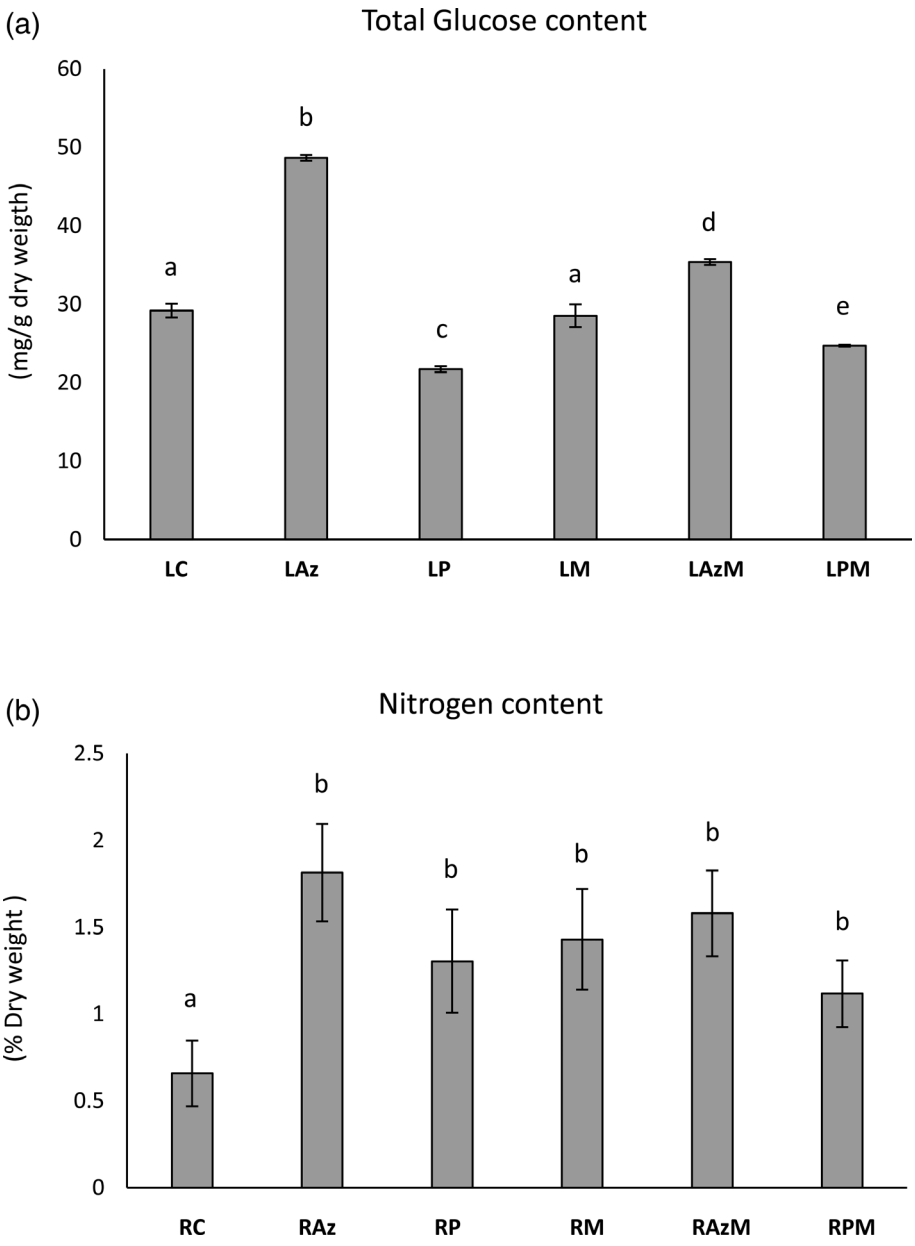

FIGURE 4 Total glucose and nitrogen (N) contents of wheat leaves and roots, respectively. (a, b) Total glucose content of leaves (a) and N content of roots (b) of C, Az, P, M, AzM, and PM wheat plants harvested at 50 dpi. Data represented as mean ± SD ($n \geq 3$) were subjected to a one-way ANOVA. Different lowercase letters indicate significant differences ($p < .05$; Tukey's test)

Proteomic data showed that *P. graminis* inoculation also had a substantial impact on primary metabolism (glycolysis, tricarboxylic acid cycle and aerobic respiration) in roots and leaves (Figures 3 and Tables S3–S6). In the LP sample, DAPs related to photosynthesis did not showed a clear pattern (Table S4).

Similar to Az plants, *P. graminis*-inoculated plants showed significantly higher concentrations of N and almost all amino acids than C plants, particularly in the roots (Figure 4b and Table S6). In P plants, the more efficient N uptake could be due to the increased abundance of the high-affinity nitrate transporter NAR2 and its activator NRT2. The abundance of the wheat ortholog of rice ammonium-inducible transporter 1–2 (OsAMT1-2) was also increased in RP sample (Figure S6 and Table S5).

Overall, most of these proteomic changes affecting respiration, photosynthesis, N assimilation and mineral nutrition mirror the differential growth response of wheat upon PGPB inoculation, as illustrated in Figure 1, with a significant systemic effect of only *A. brasilense* on plant growth.

3.5 | AMF plays a dominant role in plant roots upon binary association with PGPB

We previously showed that *F. mosseae* elicits a significant proteomic change in wheat roots and leaves during colonization (Fiorilli et al., 2018). Consistent with this observation, AzM and PM samples showed high numbers of DAPs; RAzM versus RC and RP versus RC comparisons revealed 709 and 1,055 DAPs, respectively (Tables S7 and S8), whereas LAzM versus LC and LPM versus LC comparisons revealed 504 and 808 DAPs, respectively (Tables S9 and S10, Figure S7).

Venn diagrams showed a specific contribution by *F. mosseae* in the roots of co-inoculated plants, mainly AzM plants (Figure S7b,d). These data are consistent with our previous proteomic data showing that *F. mosseae* has a stronger local but a weaker systemic impact on wheat (Fiorilli et al., 2018). In roots, inoculation with *F. mosseae* alone or together with *A. brasilense* or *P. graminis* led to an increased abundance of 196 proteins, several of which have been previously shown to increase in abundance during mycorrhization (Fiorilli et al., 2018). In particular, we found increased levels of key enzymes involved in glycolysis and the pentose phosphate pathway (glyceraldehyde-3-phosphate dehydrogenase, pyruvate kinase, and 6-phosphogluconate dehydrogenase), fatty acid biosynthesis and metabolism (plastid acetyl-CoA carboxylase and 3-oxoacyl-[acyl-carrier-protein] reductase, GDSL esterase/lipase), and mineral nutrition (OsAMT3;1 homolog). In addition, we detected significant up-regulation of some proteins involved in plant defense, including one acidic endochitinase protein, cysteine-rich receptor-like protein kinase 25 (CRK25), and some Germin-like proteins (GLPs).

Venn diagrams also showed that most DAPs were exclusively expressed in AzM and PM plants. This trend was mainly detected in leaves (Figure S7a,c). In fact, GO enrichment analysis showed that oxidative phosphorylation, response to oxidative stress, photosynthesis and response to abiotic stimulus were among the up-regulated biological processes in the LAzM versus LPM comparison. Ribosome biogenesis, translation and gene expression were down-regulated processes (Table S11 and Figure S8).

Altogether, our results revealed that organ-specific proteomic changes in AMF-inoculated wheat plants (Fiorilli et al., 2018) are mostly maintained upon binary inoculation. This suggests that the AMF plays a dominant role in the root protein profile.

3.6 | Defense proteins are induced locally and systemically during bipartite and tripartite interactions

Some rhizosphere-associated beneficial bacteria trigger a plant immunization phenomenon, called induced systemic resistance (ISR), thus priming the plant immune system (Pieterse et al., 2014). To verify whether *A. brasilense* and *P. graminis* possess the tools to elicit immune system priming in wheat, we first examined the enriched GO terms involved in plant–microbe interactions. Whereas the 'response to wounding' was one of the up-regulated GO enriched categories in RAz samples, the DAPs enriched in the category 'response to bacterium' showed a decrease, in LAz samples (Figure 3). In particular, we found reduced abundance of two chitinases, two pathogenesis-related (PR) proteins, and one protein (A0A3B6BXY2) highly similar to the Arabidopsis heat stable 1 (HS1) protein, which exhibits antibacterial activity (Park et al., 2007). This decrease in the abundance of defense-related proteins in leaves could at least partly explain the susceptibility of Az plants to *X. translucens* infection in leaf-clipping tests (Figure 2). The sucrose transporter SUT2D specifically induced by *Azospirillum* (Table S2) in wheat leaves could also play a role in the susceptibility of Az plants to pathogen infection. *Xanthomonas* TAL effectors usually target SWEET family sugar transporters to sustain pathogen growth (Verdier et al., 2012).

In RP samples harvested at 50 dpi, one of the enriched GO terms was 'defense response/incompatible interaction' with the induction of several defense proteins (Figure 3 and Table S5). Among them, the A0A3B6DGK2 protein, which is similar to RPM1-interacting protein 4 (RIN4), a major regulator of plant defense that plays important roles in both pathogen-associated molecular pattern (PAMP)-triggered immunity (PTI) and effector-triggered immunity (ETI) (Ray, Macoy, Kim, Lee, & Kim, 2019). Additionally, lipoxygenase 1 (LOX1), 12-oxophytodienoate reductase 1 (OPR1), OPR3 and allene oxide cyclase 3 (AOC3) point to up-regulation of the biosynthesis of jasmonic acid (JA), a plant hormone that plays a key role in the biotic stress response and overall plant immunity (Pieterse et al., 1998). Moreover, RP samples showed an increased abundance of a protein (A0A3B6KT24) that is similar to the respiratory burst oxidase homolog protein D (RbohD) and is involved in the generation of reactive oxygen species (ROS) during incompatible plant–pathogen interactions (Torres, Dangl, & Jones, 2002), a CERK homolog (A0A3B6RF20) and proteins required for lignin biosynthesis, which are activated in tomato plants associated with native microbiota (Chialva et al., 2018). Lastly, *P. graminis*-inoculated plants showed an increased abundance of some proteins involved in isoprene metabolism, suggesting the up-

(a)

Protein ID	Annotation	Log2 Fold Change										
		LAz/LC	LP/LC	LM/LC	LAzM/LC	LPM/LC	LX/LC	LAzX/ LC	LPX/LC	LMX/LC	LAzMX/LC	LPMX /LC
DEFENSE												
A0A3B6RIN3	Phospholipase D	0.1	-0.1	-0.3	5.8*	6.2*	-0.1	5.6*	6.5*	-0.6	5.5*	5.7*
A0A077RUB2	Phospholipase A1-II 5	-0.4	0.0	0.4	0.6	1.1*	0.4	0.1	0.2	0.4	0.2	1.4*
A0A3B5Z2B1	Phospholipase A1-II 7	-3.2*	-6.3*	0.7	0.9	-7.2*	0.2	-1.9*	-1.6*	1.1*	2.6*	0.2
A0A3B5YZC4	Phospholipase A1-II 7	-0.1	0.4	0.8	0.4	-0.8	-0.4	0.3	-0.9	0.1	5.8*	-0.3
A0A3B5ZXW7	Phospholipase A1-II 7	-0.7	0.2	0.2	0.3	1.1*	0.3	0.0	1.3*	0.6	1.9*	0.8
A0A3B6QM37	Allene oxide cyclase 3	0.7	0.8	-0.2	1.0*	0.8	0.3	0.9	0.8	0.4	1.4*	1.0*
A0A3B6NUZ0	Allene oxide cyclase	5.2*	5.5*	-1.0*	5.4*	5.9*	4.5*	5.3*	5.0*	-0.7	5.3*	6.1*
T1WRJ1	Allene oxide synthase	-0.2	-0.2	-0.2	-0.4	-0.1	-0.2	-0.4	0.4	-0.1	5.3*	3.4*
A0A3B6HS52	Allene oxide synthase	-1.2*	-0.8	-1.0*	4.3*	-0.6	-0.6	-0.3	-0.9	-0.9	5.6*	-0.9
A0A3B6MID4	Lipoxygenase	-0.4	-0.9	6.7*	7.2*	6.6*	7.4*	5.6*	4.8*	6.8*	8.5*	6.7*
A0A341WW51	Lipoxygenase	0.4	5.5*	-0.7	5.4*	6.4*	6.8*	5.1*	8.0*	0.7	10.2*	4.6*
A0A3B6KC55	Lipoxygenase	-1.8*	-0.3	0.0	1.0*	0.2	0.5	0.1	-0.5	-0.3	2.2*	0.6
A0A3B6DM57	Lipoxygenase	-1.6*	-0.6	0.2	1.0*	0.2	0.1	-0.1	-0.1	-0.3	2.1*	0.6
A0A3B6CF89	Lipoxygenase	-1.2*	-0.3	-0.1	0.7	-0.1	0.0	-0.4	-0.5	-0.4	1.8*	0.3
C6K7G3	Lipoxygenase	4.7*	4.2*	0.1	5.3*	0.5	0.5	0.8	-0.3	-0.1	6.2*	4.3*
A0A3B6LF12	Lipoxygenase	-0.5	6.4*	6.7*	7.1*	7.3*	7.0*	6.8*	6.7*	6.6*	9.5*	7.0*
A0A3B6PJ16	Lipoxygenase	-2.5*	2.2*	-7.2*	0.1	1.4*	2.5*	1.9*	3.6*	-4.2*	6.2*	-0.8
A0A3B5Y002	Similar to BSK1, BR-signaling kinase 1	1.0*	0.4	0.8	6.6*	7.2*	0.5	6.8*	6.6*	0.9	6.6*	7.0*
W5BC19	NDR1/HIN1-like protein 12	-0.3	-0.5	-0.9	3.8*	4.9*	-0.4	4.2*	2.8*	-0.8	4.1*	4.1*
A0A3B5Y5B5	Pathogenesis-related protein 4	-0.5	0.1	0.4	5.3*	4.5*	-0.2	5.1*	4.9*	4.1*	5.7*	5.3*
A0A3B6CFS9	Superoxide dismutase	0.7	0.4	0.5	9.6*	9.2*	8.3*	0.1	8.8*	0.9	9.1*	9.6*
H9CDF8	Hypersensitive induced reaction protein 3	6.4*	0.1	0.1	-0.1	7.1*	0.5	-0.3	0.9	-0.6	-0.2	7.1*
A0A3B6IWD4	Chitin elicitor-binding protein	0.1	0.2	-0.4	0.0	1.0*	-0.1	0.4	0.3	-0.3	0.1	0.8
Q53WS1	Alpha 1 purothionin	-0.2	0.0	-0.2	0.1	0.6	0.3	0.6	0.8	0.4	0.3	7.0*
H9CDF6	Hypersensitive induced reaction protein 1	1.1*	0.2	-0.2	0.9	2.2*	0.1	0.8	0.8	0.1	0.9	2.2*
A0A3B6LR15	Endoglucanase	5.7*	5.4*	0.1	0.4	6.1*	5.3*	-0.4	5.3*	0.4	0.1	5.5*
G3E8E2	Aquaporin 8	1.5*	-6.8*	-0.4	1.2*	1.7*	-0.2	-7.1*	-0.2	-0.3	-0.2	2.0*
A0A1D5UQF7	Aquaporin	1.0*	-0.1	-0.7	1.2*	2.8*	-0.5	0.6	0.7	0.1	1.3*	2.8*
A0A3B6LGA8	Riboflavin synthase alpha chain	0.4	-0.1	-0.1	-0.2	0.5	-0.4	0.2	0.7	0.0	0.0	1.2*
A0A3B6SC01	Caffeoyl-CoA O-methyltransferase	6.0*	6.4*	-0.2	0.3	0.6	0.8	0.6	0.6	0.1	-0.5	1.3*

(b)

Protein ID	Annotation	Log2 Fold Change										
		LAz/LC	LP/LC	LM/LC	LAzM/LC	LPM/LC	LX/LC	LAzX/ LC	LPX/LC	LMX/LC	LAzMX/LC	LPMX /LC
CELL WALL												
W5EIQ2	3-ketoacyl-CoA synthase	0.5	-0.3	-0.3	0.3	1.4*	-0.3	-6.3*	-0.9	-0.6	0.0	1.4*
A0A3B6U7D2	3-ketoacyl-CoA synthase	-0.6	-1.0*	-0.4	-0.4	-0.6	-1.0*	-0.4	-0.6	-0.7	0.0	6.0*
A0A3B6DKP9	Bifunctional inhibitor/lipid-transfer protein	-2.1*	-1.2*	0.8	-0.8	0.7	0.6	-0.8	-0.3	0.6	-1.8*	0.8*
A0A3B6IP95	Arabinoxylan arabinofuranohydrolase	0.1	-0.1	0.3	0.7	0.8*	0.3	0.2	0.2	0.2	0.2	0.9*
EPIGENETIC REGULATION												
A0A3B6CD30	Histone H1	-0.1	-1.2*	0.7	-0.2	1.4*	0.0	-1.6*	-1.7*	0.4	-1.3*	1.0*
Q9SWU2	Histone H1 WH1A.2	-0.3	-0.3	1.1*	0.0	1.6*	0.3	-0.8	0.2	0.2	-0.5	1.4*
A0A3B5ZWS7	Histone H2B	0.4	-0.2	7.8*	0.0	0.0	6.2*	0.2	0.8	6.4*	-0.4	6.5*
A0A3B6QC63	Histone H2B	-3.0*	5.9*	0.2	5.7*	-2.3*	6.1*	6.8*	5.8*	0.5	5.7*	-1.9*
TRANSLATION												
A0A1D6DK86	40S ribosomal protein S24	0.7	0.6	1.0*	0.6	2.6*	0.3	-6.9*	1.4*	0.7	0.5	1.7*
W5HZ68	40S ribosomal protein S27	-1.8*	-1.9*	-0.2	-1.0*	1.2*	-1.4*	-2.7*	-2.5*	-0.8	-0.7	1.7*
A0A075TNZ7	50S ribosomal protein L2, chloroplastic	0.5	0.3	1.5*	1.0*	2.2*	0.1	0.3	0.7	0.8	0.8	2.1*
A0A3B5YQM4	50S ribosomal protein L28, chloroplastic	-1.1*	-1.5*	0.8	-5.5*	1.8*	-6.1*	-6.1*	-6.6*	-0.1	-6.2*	2.8*
A0A0C4BIR6	60S ribosomal protein L10-2	-0.1	-0.4	1.0*	0.5	1.6*	0.3	-0.5	-0.7	0.8	0.1	1.6*
A0A3B6SDH0	60S ribosomal protein L13	0.3	0.8	0.4	0.7	6.9*	0.5	0.5	1.0*	0.7	1.0*	6.7*
A0A3B6RJP2	60S ribosomal protein L13	-0.9	-0.9	0.2	3.9*	5.1*	0.2	0.7	-0.4	0.1	-1.0*	4.7*
W5BRK9	60S ribosomal protein L13a-4	-0.6	-1.4*	0.8	-0.6	2.7*	0.0	-1.9*	0.0	-0.1	-0.5	2.1*
W5CDW4	60S ribosomal protein L24	-0.2	-7.0	1.1*	0.1	2.3*	-0.3	-0.3	0.4	0.0	0.0	1.8*
A0A3B6GQI2	60S ribosomal protein L26-1	0.7	0.3	0.6	1.1*	1.9*	0.3	0.3	-0.1	0.5	0.4	2.0*
D8L9P6	60S ribosomal protein L37a	1.1*	0.9	0.8	1.5*	2.3*	0.0	1.0*	0.7	0.3	1.1*	2.5*
W5FEV1	60S ribosomal protein L7-2	-0.1	-0.5	0.6	0.4	1.6*	-0.1	-0.4	-0.1	0.1	0.4	1.4*
W5ECL2	60S ribosomal protein L8	0.4	0.1	0.7	0.9	1.9*	-0.1	0.3	0.6	0.2	0.8	1.8*
Q5I7K4	Ribosomal protein L17	0.0	0.2	0.7	0.8	1.8*	-0.3	0.1	0.6	0.3	0.7	1.6*
A0A3B6C2W3	Ribosomal protein L19	0.6	0.4	0.6	5.2*	5.8*	0.2	0.8	0.9	0.4	1.0*	5.2*
A0A3B6I211	Ribosomal protein S25	0.9	0.9	0.5	1.0*	1.7*	0.0	0.0	0.9	0.4	0.3	2.4*
A0A2Z6C7P4	Ribosomal protein S4	1.4*	1.0*	1.9*	2.6*	4.1*	0.7	1.2*	1.4*	1.5*	2.2*	3.9*
A0A2Z6C8D2	Ribosomal protein S8	0.5	0.1	0.9	0.8	2.4*	0.3	-0.5	0.3	0.6	0.3	1.9*
A0A3B6LWE2	rRNA N-glycosidase	-0.2	-0.5	0.1	-0.5	-0.7	0.3	-0.7	0.1	-0.1	-0.1	5.8*
A0A3B6LVN2	Ribosomal protein S5 family protein	-0.1	-0.4	0.4	-0.3	2.1*	-0.2	-0.6	0.4	-0.1	-0.4	1.8*
A0A1D5Z340	Ribosomal protein L7Ae	1.1*	0.4	0.4	1.5*	2.9*	0.2	1.1*	0.7	0.2	1.3*	2.6*
A0A3B6B8T0	30S ribosomal protein S17, chloroplastic	-1.5*	-1.6*	0.5	-1.0*	2.0*	-0.9	-6.9*	-2.1*	-1.4*	0.1	2.5*

FIGURE 5 Legend on next page.

regulation of pathways involved in plant defense. These data support the hypothesis that similar to other PGPB (Pieterse et al., 1998) and unlike *A. brasilense*, *P. graminis* elicits an immune response in the roots but does not elicit strong ISR at 50 dpi in the leaves against *X. translucens* infection (Figure 2).

To describe the systemic bioprotective effect of AMF and PGPB co-inoculation in wheat, we performed LAzM versus LAz and LPM versus LP comparisons (Tables S12 and S13). Our analysis showed an increase in several DAPs, putatively involved in the biotic stress response, in both LAzM and LPM samples (Figure 5a). Among these DAPs, we found proteins either involved in JA biosynthesis, such as a phospholipase D, three LOXs, and an AOC, or induced by JA, such as a dirigent protein, PR4 (wheat protein) (Desmond et al., 2005) and OsMPK1 (Singh & Jwa, 2013). Moreover, we observed an increase in the abundance of other proteins involved in signaling of the plant immune response, such as the homolog of brassinosteroid (BR)-signaling kinase 1 (BSK1) (Shi et al., 2013) and a calcium-transporting ATPase, whose homolog (ACA8) is required for limiting the growth of virulent bacteria in Arabidopsis (Frei dit Frey et al., 2012). Another protein, whose expression was highly induced in LPM and LAzM samples, was manganese superoxide dismutase 1 (Mn-SOD1), which belongs to the polyphyletic family of enzymes and protect cells from reactive superoxide radical-induced damage, thus conferring increased stress tolerance (Wang et al., 2017).

Overall, this analysis revealed some unexpected features: *A. brasilense* alone down-regulates plant defense (which is consistent with the observed disease susceptibility phenotype shown in Figure 2), while single inoculations of *P. graminis* and *F. mosseae* trigger a similar number of proteins involved in the plant immune response in an organ-dependent way. Co-inoculation of wheat plants with the AMF and *A. brasilense* or *P. graminis* elicits the plant immune response not only in LPM but also in LAzM samples, at least in the short term, suggesting that both microbial pairs (AMF–*A. brasilense* and AMF–*P. graminis*) induce a priming response at least at the proteome level (Figure 5a).

3.7 | Microbial pairs modulate wheat response to *X. translucens* by inducing different proteomic changes

Leaf inoculation of M, Az, P and C plants with *X. translucens* revealed that pathogen susceptibility detected in the leaves of LAzX plants was alleviated by the presence of mycorrhizal colonization at 4 dpc (based on the LAzMX versus LAzX comparison) (Figure 2a). To decipher the main proteins responsible for the reduction of symptoms at 4 dpc, we analyzed the DAPs identified in the LAzMX versus LAzX and LAzMX versus LMX comparisons (Tables S14 and S15).

The up-regulated proteins included those involved in JA biosynthesis and response. Several LOXs and two lipases including phospholipase A1-II and phospholipase D, which generate fatty acid substrates for JA biosynthesis (Browse, 2009), were highly induced in the LAzMX versus LAzX and LAzMX versus LMX comparisons (Ishiguro, Kawai-Oda, Ueda, Nishida, & Okada, 2001; Lee & Park, 2019; Wang et al., 2000; Wasternack & Hause, 2013) (Figure 5a, Tables S14 and S15). In addition, two allene oxide synthase (AOS) enzymes, which catalyze the first step in the JA biosynthesis pathway, and two AOCs, which are committed for the second step in this pathway (Schaller & Stintzi, 2009), were highly induced in LAzMX samples (Figure 5a) compared with LAzX and LMX samples. In addition, we found that two JA-induced dirigent-like proteins, which act downstream of the JA biosynthesis pathway, were induced in LAzMX samples. This increase of proteins involved in JA biosynthesis was also observed in LPMX samples (Figure 5a).

Our results showed that *A. brasilense*–AMF and *P. graminis*–AMF interactions amplified JA signaling during pathogen attack. In addition, proteins involved in biotic stress, which were induced during *A. brasilense*–AMF and *P. graminis*–AMF interactions in LAzM and LPM samples, respectively (Figure 5a), were also recruited during *X. translucens* infection, as testified by their higher abundance in LAzMX and LPMX samples, respectively.

These proteomic data correlate with the reduced lesion length observed at the early time point (4 dpc) in AzMX plants with respect to AzX plants. However, at 26 dpc, a significant reduction in lesion size resulted only in MX and PMX plants compared with CX plants (Figure 2b). These data suggest that when co-inoculated with *A. brasilense*, the bioprotective effect exerted of *F. mosseae* is transient and probably related to prompt induction of the JA response.

Further analysis is needed to clarify the molecular changes during the later stage of pathogen attack under different conditions. However, the proteomic profile of LAzMX samples was very different from that of LPMX samples (799 DAPs; Table S16). Among the most abundant proteins identified in the LAzMX versus LPMX comparison, we found proteins involved in the response to abiotic stimulus and oxidative stress, while those implicated in translation, ribosome biogenesis, gene expression were down-regulated. A similar pattern was already observed in the LAzM versus LPM comparison (Figure S8).

Overall, these data highlight the intricate network of processes that regulate wheat–PGPB–AMF–pathogen interactions (as observed in LAzMX and LPMX samples). However, elicitation of defense priming in the proteome of LAzM and LPM samples does not necessarily lead to better performance once the plant is under pathogen attack.

4 | DISCUSSION

Wheat, one of the earliest food crops to be domesticated, is currently the second most widely cultivated crop in the world and one of the most important grain sources for humans. Given the increasing

FIGURE 5 Heat map of the main DAPs involved in plant defense (a) and in cell wall production, epigenetic regulation, translation (b) found in wheat leaves inoculated with PGPB and/or AM fungus (AMF) and treated with or without *X. translucens*. Log_2fold-change (Log_2FC) values indicate the changes in protein abundance with respect to the control. Red and blue indicate maximum and minimum values, respectively. Asterisks indicate significant differences (ANOVA FDR < 0.01; Tukey's test) [Colour figure can be viewed at wileyonlinelibrary.com]

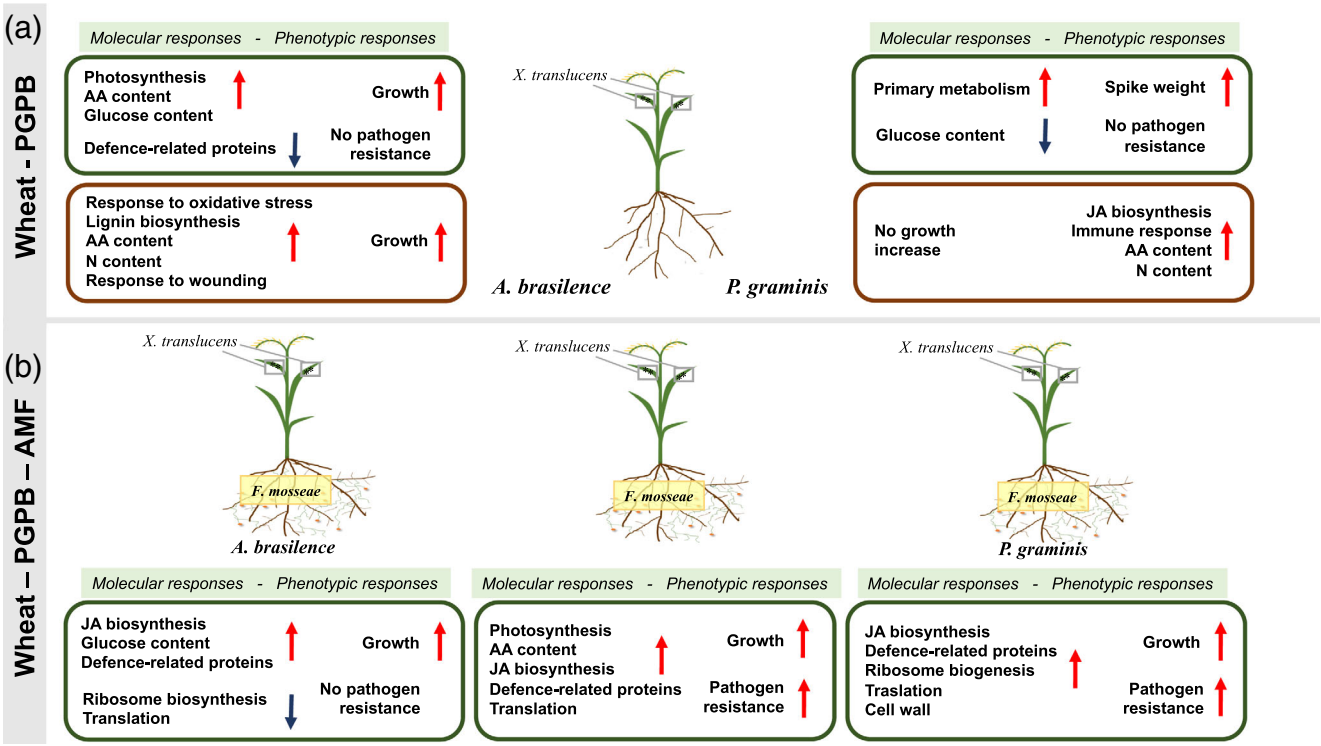

FIGURE 6 (a) Scheme showing the molecular and phenotypic responses of non-mycorrhizal wheat colonized by *A. brasilence* (left side) and *P. graminis* (right side). (b) Scheme showing the molecular and phenotypic responses of mycorrhizal (*F. mosseae*) wheat alone (center) or colonized by *A. brasilence* (left side) and *P. graminis* (right side). The green boxes include the effects on the leaves while the brown ones include the effects on the roots [Colour figure can be viewed at wileyonlinelibrary.com]

relevance of plant microbiota, many researches have described wheat-associated microbiota by considering the effects in different organs as well as in grain production. The results of this study illustrate how proteomic changes in wheat plants depend on the inoculum composition (single or multiple microbes) and the organ under study, and lead to differential growth effects and pathogen resistance. All analyses revealed that the AMF was the crucial driver of plant growth and defense priming under our growth conditions (low P). However, the overall changes induced by the AMF–PGPB consortium can interfere with the final mycorrhizal-induced resistance (MIR) outcome (Figure 6).

4.1 | Effect of beneficial microbes on wheat growth is organ- and microbial identity-dependent

In addition to their N-fixing ability, *Azospirillum* spp. exhibit a remarkable capacity to benefit a wide range of plant species by activating multiple mechanisms (Fukami, Cerezini, & Hungria, 2018); however, the available omics data are limited to the effects of *A. brasilense* inoculation on roots (Drogue et al., 2014; Spaepen, Bossuyt, Engelen, Marchal, & Vanderleyden, 2014). In this study, we showed that the higher root and shoot biomass of plants colonized by *A. brasilense* is supported by the sustained activation of the main metabolic processes (respiration, photosynthesis and N assimilation), while the roots act as a strong sink for nutrients, such as hexoses and amino acids. These results are consistent with the findings of Zeffa and colleagues, who showed that *A. brasilense* promotes plant growth in maize by enhancing the plant photosynthetic potential or by increasing the N use efficiency (Zeffa et al., 2019) On the other hand, *P. graminis* did not efficiently increase the root and shoot biomass of wheat plants but increased the spike biomass.

Wheat actively responds to *P. graminis* inoculation by eliciting many metabolic processes, which involve a higher number of DAPs compared with those induced by *A. brasilense*. Some of these processes were, however, common to the two bacterial species (e.g., processes involved in ROS scavenging) as well described for many other PGPB (Fukami et al., 2018).

Wheat responds well to AMF, particularly *F. mosseae* (Fiorilli et al., 2018). The wheat–PGPB–AMF tripartite interaction led to intensive proteomic changes where nutrient transporters and many enzymes involved in primary and secondary metabolism, protein biosynthesis and ROS homeostasis were elicited.

Overall, plant growth experiments, nutrient quantification and proteomic analyses demonstrated that the AMF plays a leading role in tripartite interactions, particularly in the root, while PGBP (at least *Azospirillum*) affects systemic growth, as evident from the leaf proteome.

4.2 | The bioprotective effect of the AMF is modulated by the nature of the co-inoculated PGPB

PGPB are considered essential components of the plant microbiota because of their ability to improve plant growth via multiple mechanisms, including plant health protection (Berendsen, Pieterse, & Bakker, 2012; Lugtenberg et al., 2016). *Azospirillum* is not a typical biocontrol agent, despite studies showing its ability to increase pathogen resistance in plants (Bashan & de-Bashan & de Bashan, 2002; Kusajima et al., 2018; Tortora, Díaz-Ricci, & Pedraza, 2012; Yasuda, Isawa, Shinozaki, Minamisawa, & Nakashita, 2009). On the other hand, some *Paraburkholderia* taxa, such as *P. phytofirmans*, induce resistance against a broad range of plant pathogens by inducing plant-mediated responses in aerial organs (Miotto-Vilanova et al., 2016). Proteomic analysis of wheat plants inoculated with a single microbe showed that proteins involved in plant defense were down-regulated in LAz samples. Moreover, according to the 'pathogen starvation' model, which links plant resistance with soluble sugars (Bezrutczyk et al., 2018), the high sugar and amino acid contents of LAz leaves coupled with an enhanced abundance of sugar transporters could guarantee a nutrient-rich niche for the pathogen. Under these conditions, the plant could not activate any defense mechanisms, notwithstanding a light improvement in the presence of the AMF at 4 dpc.

P. graminis induced diverse proteomic changes in roots characterized by an increase in the abundance of proteins involved in microbe-associated molecular pattern (MAMP) perception, PTI and ETI regulation (RIN4), ROS production and detoxification, lignin biosynthesis and isoprene metabolism. These findings suggest that *P. graminis* elicits an immunomodulatory response; however, this does not lead to ISR.

The protein profiles clearly indicate the capacity of mycorrhizal plants, associated with PGPB, to increase the number of defense-related proteins in leaves in the absence of the pathogen, and an augmented capacity to express these proteins upon pathogen infection (Figure 5a). The up-regulation of JA biosynthesis proteins was a key finding because this hormone is considered the first regulator of the plant immune response (Hickman et al., 2017; Pieterse et al., 1998). Several studies reported that AM symbiosis protects plants against pathogens, suggesting that JA defense mechanisms play a key role in MIR (Jung, Martinez-Medina, Lopez-Raez, & Pozo, 2012).

AMF are a crucial component of the plant microbiota (Bonfante, Venice, & Lanfranco, 2019) and the first inducers of plant immunity. A previous study showed that co-inoculation of wheat with an AMF and *Pseudomonas* spp. (PGPB) leads to synergistic effects, priming the host immunity through chitosan-induced callose deposition (Pérez-de-Luque et al., 2017). A comparable result has been described in tomato plants grown in native soil containing multiple bacteria and AMF; MAMPs released by various microbes enhance the plant immunity, thus activating PTI markers. When challenged by pathogenic *Fusarium* spp., the tomato plants were strongly protected because of the activation of specific antifungal proteins (Chialva, Zhou, Spadaro, & Bonfante, 2018).

According to a previously proposed hypothesis (Cameron, Neal, van Wees, & Ton, 2013), JA could act as a long distance signaling molecule that in mycorrhizal wheat, and also in the presence of both PGPB species, activates the systemic priming of plant defense. However, in our system, lesion length was reduced only at the early time point (4 dpc) in AzMX plants in comparison with AzX plants. At 26 dpc, a significant reduction in lesion length was observed only in MX and PMX plants in comparison with CX plants (Figure 2b). We speculate that additional determinants induced by the AMF–PGPB interactions interfere with cellular processes, leading to MIR. Proteomic data showed that in LAzMX samples, the abundance of proteins involved in ribosome biogenesis and gene expression decreased compared with their abundance in LMX and LBMX samples (Figure 5b). Ribosomal genes are highly responsive to stress and signaling molecules, indicating that the encoded proteins play roles in stress amelioration, besides house-keeping. The instantaneous up-regulation of ribosomal genes in response to stress might function as a prompt defense response (Moin et al., 2016). In addition, a reduction in HMGA subfamily transcription factor and H2B and H1 histones could affect the transcription of defense-related genes (Isaac, Hartney, Druffel, & Hadwiger, 2009). Finally, a reduction in the abundance of two proteins involved in stomata regulation, H1.3 and ubiquitin-specific protease 24 (Rutowicz et al., 2015; Zhao et al., 2016), and some proteins involved in cuticular wax production, could promote leaf pathogen invasion in AzMX plants.

5 | CONCLUSION

Plant-associated microbiota hold great promise for the development of sustainable crop systems, and this can be guaranteed by the use of SynComs (Kong, Hart, & Liu, 2018). However, results obtained from on-field microbiota census and those obtained using reductionist approaches, mostly through laboratory-based experiments, have not yet been fully integrated (Fitzpatrick et al., 2020). Our results suggest that beneficial microbes have different impacts on plants, at least in wheat, and the plant growth-promoting effects of beneficial microbes are not always accompanied by enhanced pathogen resistance, as shown by *A. brasilense* inoculation (Figure 6). On the other hand, a bacterium that does not show strong growth-promoting effect, such as *P. graminis*, may be more effective against pathogen attack, if associated with an AMF (Figure 6). Our data highlight the crucial role of AM fungi, which are often absent in SynComs, as well as the potential contrasting effects of different AMF–PGPB consortia on plant defense. In a wider context, these findings suggest that SynCom efficiency should be validated by checking the outcome of the interaction under different conditions (microbe-microbe interactions; nutritional

status, plant life cycle and biotic stress) before their exploitation for crop growth.

ACKNOWLEDGMENTS

This work was supported by the MIC-CERES ('Microbial eco-compatible strategies for improving wheat quality traits and rhizospheric soil sustainability') Project (FC Project ID 2013–1888; AF Project ID 1301–003) jointly supported by the Agropolis Foundation (through the 'Investissements d'avenir' program, with the reference number ANR-10-LABX-0001-01) and Fondazione Cariplo. The authors thank the Functional Genomics Center Zurich (FGCZ) for providing highly valuable technical support.

CONFLICT OF INTEREST

The authors have no conflict of interest to declare.

AUTHOR CONTRIBUTIONS

V.F., D.G.S., P.B., L.M. and C.V designed the study; V.F., D.G.S., M.N. and D.G. carried out the majority of experiments; G.D., M.M. and C.V performed the bioinformatic analysis of proteomic data; C.V., V.F., P.B. L.M., F.W.-D. and M.B. interpreted the data and wrote the manuscript.

DATA AVAILABILITY STATEMENT

Data available on request from the authors.

ORCID

Candida Vannini https://orcid.org/0000-0002-5196-6142
Valentina Fiorilli https://orcid.org/0000-0001-9805-1559
Milena Marsoni https://orcid.org/0000-0003-0613-1581

REFERENCES

Baez-Rogelio, A., Morales-García, Y. E., Quintero-Hernández, V., & Muñoz-Rojas, J. (2017). Next generation of microbial inoculants for agriculture and bioremediation. *Microbial Biotechnology*, *10*(1), 19–21. https://doi.org/10.1111/1751-7915.12448

Bashan, Y., & de Bashan, L. E. (2002). Protection of tomato seedlings against Infection by *Pseudomonas syringae* pv. tomato by using the plant growth-promoting bacterium *Azospirillum brasilense*. *Applied and Environmental Microbiology*, *68*(6), 2637. https://doi.org/10.1128/AEM.68.6.2637-2643.2002

Berendsen, R. L., Pieterse, C. M., & Bakker, P. A. (2012). The rhizosphere microbiome and plant health. *Trends in Plant Science*, *17*(8), 478–486. https://doi.org/10.1016/j.tplants.2012.04.001

Bezrutczyk, M., Yang, J., Eom, J.-S., Prior, M., Sosso, D., Hartwig, T., … Frommer, W. B. (2018). Sugar flux and signaling in plant–microbe interactions. *The Plant Journal*, *93*(4), 675–685. https://doi.org/10.1111/tpj.13775

Bonfante, P., Venice, F., & Lanfranco, L. (2019). The mycobiota: Fungi take their place between plants and bacteria. *Current Opinion in Microbiology*, *49*, 18–25. https://doi.org/10.1016/j.mib.2019.08.004

Browse, J. (2009). Jasmonate passes muster: A receptor and targets for the defense hormone. *Annual Review of Plant Biology*, *60*(1), 183–205. https://doi.org/10.1146/annurev.arplant.043008.092007

Bulgarelli, D., Rott, M., Schlaeppi, K., Ver Loren van Themaat, E., Ahmadinejad, N., Assenza, F., … Schulze-Lefert, P. (2012). Revealing structure and assembly cues for Arabidopsis root-inhabiting bacterial microbiota. *Nature*, *488*(7409), 91–95. https://doi.org/10.1038/nature11336

Cameron, D. D., Neal, A. L., van Wees, S. C., & Ton, J. (2013). Mycorrhiza-induced resistance: More than the sum of its parts? *Trends in Plant Science*, *18*(10), 539–545. https://doi.org/10.1016/j.tplants.2013.06.004

Carvalho, T. L. G., Balsemão-Pires, E., Saraiva, R. M., Ferreira, P. C. G., & Hemerly, A. S. (2014). Nitrogen signalling in plant interactions with associative and endophytic diazotrophic bacteria. *Journal of Experimental Botany*, *65*(19), 5631–5642. https://doi.org/10.1093/jxb/eru319

Chialva, M., Salvioli di Fossalunga, A., Daghino, S., Ghignone, S., Bagnaresi, P., Chiapello, M., … Bonfante, P. (2018). Native soils with their microbiotas elicit a state of alert in tomato plants. *The New Phytologist*, *220*(4), 1296–1308. https://doi.org/10.1111/nph.15014

Chialva, M., Zhou, Y., Spadaro, D., & Bonfante, P. (2018). Not only priming: Soil microbiota may protect tomato from root pathogens. *Plant Signaling & Behavior*, *13*(8), e1464855. https://doi.org/10.1080/15592324.2018.1464855

Desmond, O. J., Edgar, C. I., Manners, J. M., Maclean, D. J., Schenk, P. M., & Kazan, K. (2005). Methyl jasmonate induced gene expression in wheat delays symptom development by the crown rot pathogen *Fusarium pseudograminearum*. *Physiological and Molecular Plant Pathology*, *67*(3), 171–179. https://doi.org/10.1016/j.pmpp.2005.12.007

Drogue, B., Sanguin, H., Chamam, A., Mozar, M., Llauro, C., Panaud, O., … Wisniewski-Dyé, F. (2014). Plant root transcriptome profiling reveals a strain-dependent response during Azospirillum-rice cooperation. *Frontiers in Plant Science*, *5*, 607. https://doi.org/10.3389/fpls.2014.00607

Du, Z., Zhou, X., Ling, Y., Zhang, Z., & Su, Z. (2010). agriGO: A GO analysis toolkit for the agricultural community. *Nucleic Acids Research*, *38*(Web Server issue), W64–W70. https://doi.org/10.1093/nar/gkq310

Durán, P., Thiergart, T., Garrido-Oter, R., Agler, M., Kemen, E., Schulze-Lefert, P., & Hacquard, S. (2018). Microbial interkingdom interactions in roots promote *Arabidopsis* survival. *Cell*, *175*(4), 973.e914–983.e914. https://doi.org/10.1016/j.cell.2018.10.020

Eom, J. S., Cho, J. I., Reinders, A., Lee, S. W., Yoo, Y., Tuan, P. Q., … Jeon, J. S. (2011). Impaired function of the tonoplast-localized sucrose transporter in rice, OsSUT2, limits the transport of vacuolar reserve sucrose and affects plant growth. *Plant Physiology*, *157*(1), 109–119. https://doi.org/10.1104/pp.111.176982

Fernie, A. R., & Yan, J. (2019). De novo domestication: An alternative route toward new crops for the future. *Molecular Plant*, *12*(5), 615–631. https://doi.org/10.1016/j.molp.2019.03.016

Fiorilli, V., Vannini, C., Ortolani, F., Garcia-Seco, D., Chiapello, M., Novero, M., … Bonfante, P. (2018). Omics approaches revealed how arbuscular mycorrhizal symbiosis enhances yield and resistance to leaf pathogen in wheat. *Scientific Reports*, *8*(1), 9625. https://doi.org/10.1038/s41598-018-27622-8

Fitzpatrick, C. R., Salas-González, I., Conway, J. M., Finkel, O. M., Gilbert, S., Russ, D., … Dangl, J. L. (2020). The plant microbiome: From ecology to reductionism and beyond. *Annual Review of Microbiology*, *74*(1), 81–100. https://doi.org/10.1146/annurev-micro-022620-014327

Frei dit Frey, N., Mbengue, M., Kwaaitaal, M., Nitsch, L., Altenbach, D., Häweker, H., … Robatzek, S. (2012). Plasma membrane calcium ATPases are important components of receptor-mediated signaling in plant immune responses and development. *Plant Physiology*, *159*(2), 798–809. https://doi.org/10.1104/pp.111.192575

Fukami, J., Cerezini, P., & Hungria, M. (2018). Azospirillum: Benefits that go far beyond biological nitrogen fixation. *AMB Express*, *8*(1), 73. https://doi.org/10.1186/s13568-018-0608-1

Garcia-Seco, D., Chiapello, M., Bracale, M., Pesce, C., Bagnaresi, P., Dubois, E., … Koebnik, R. (2017). Transcriptome and proteome analysis reveal new insight into proximal and distal responses of wheat to foliar infection by *Xanthomonas translucens*. *Scientific Reports*, *7*(1), 10157. https://doi.org/10.1038/s41598-017-10568-8

Hacquard, S., Garrido-Oter, R., González, A., Spaepen, S., Ackermann, G., Lebeis, S., … Schulze-Lefert, P. (2015). Microbiota and host nutrition across plant and animal kingdoms. *Cell Host & Microbe*, *17*(5), 603–616. https://doi.org/10.1016/j.chom.2015.04.009

Hacquard, S., Spaepen, S., Garrido-Oter, R., & Schulze-Lefert, P. (2017). Interplay between innate immunity and the plant microbiota. *Annual Review of Phytopathology*, *55*, 565–589. https://doi.org/10.1146/annurev-phyto-080516-035623

Hassani, M. A., Özkurt, E., Seybold, H., Dagan, T., & Stukenbrock, E. H. (2019). Interactions and coadaptation in plant metaorganisms. *Annual Review of Phytopathology*, *57*, 483–503. https://doi.org/10.1146/annurev-phyto-082718-100008

Herrera Paredes, S., Gao, T., Law, T. F., Finkel, O. M., Mucyn, T., Teixeira, P. J. P. L., … Castrillo, G. (2018). Design of synthetic bacterial communities for predictable plant phenotypes. *PLoS Biology*, *16*(2), e2003962. https://doi.org/10.1371/journal.pbio.2003962

Hickman, R., Van Verk, M. C., Van Dijken, A. J. H., Mendes, M. P., Vroegop-Vos, I. A., Caarls, L., … Van Wees, S. C. M. (2017). Architecture and dynamics of the jasmonic acid gene regulatory network. *Plant Cell*, *29*(9), 2086–2105. https://doi.org/10.1105/tpc.16.00958

Isaac, J., Hartney, S. L., Druffel, K., & Hadwiger, L. A. (2009). The non-host disease resistance response in peas; alterations in phosphorylation and ubiquitination of HMG A and histones H2A/H2B. *Plant Science*, *177*(5), 439–449. https://doi.org/10.1016/j.plantsci.2009.07.007

Ishiguro, S., Kawai-Oda, A., Ueda, J., Nishida, I., & Okada, K. (2001). The DEFECTIVE IN ANTHER DEHISCIENCE gene encodes a novel phospholipase A1 catalyzing the initial step of jasmonic acid biosynthesis, which synchronizes pollen maturation, anther dehiscence, and flower opening in *Arabidopsis*. *Plant Cell*, *13*(10), 2191–2209. https://doi.org/10.1105/tpc.010192

Jung, S. C., Martinez-Medina, A., Lopez-Raez, J. A., & Pozo, M. J. (2012). Mycorrhiza-induced resistance and priming of plant defenses. *Journal of Chemical Ecology*, *38*(6), 651–664. https://doi.org/10.1007/s10886-012-0134-6

Kapulnik, Y., Okon, Y., & Henis, Y. (1985). Changes in root morphology of wheat caused by *Azospirillum* inoculation. *Canadian Journal of Microbiology*, *31*(10), 881–887. https://doi.org/10.1139/m85-165

Kong, Z., Hart, M., & Liu, H. (2018). Paving the way from the lab to the field: Using synthetic microbial consortia to produce high-quality crops. *Frontiers in Plant Science*, *9*, 1467. https://doi.org/10.3389/fpls.2018.01467

Kusajima, M., Shima, S., Fujita, M., Minamisawa, K., Che, F.-S., Yamakawa, H., & Nakashita, H. (2018). Involvement of ethylene signaling in *Azospirillum* sp. B510-induced disease resistance in rice. *Bioscience, Biotechnology, and Biochemistry*, *82*(9), 1522–1526. https://doi.org/10.1080/09168451.2018.1480350

Kuźniar, A., Włodarczyk, K., Grządziel, J., Goraj, W., Gałązka, A., & Wolińska, A. (2020). Culture-independent analysis of an endophytic core microbiome in two species of wheat: *Triticum aestivum* L. (cv. 'Hondia') and the first report of microbiota in *Triticum spelta* L. (cv. 'Rokosz'). *Systematic and Applied Microbiology*, *43*(1), 126025. https://doi.org/10.1016/j.syapm.2019.126025

Lee, H. J., & Park, O. K. (2019). Lipases associated with plant defense against pathogens. *Plant Science*, *279*, 51–58. https://doi.org/10.1016/j.plantsci.2018.07.003

Lugtenberg, B. J., Caradus, J. R., & Johnson, L. J. (2016). Fungal endophytes for sustainable crop production. *FEMS Microbiology Ecology*, *92*(12). https://doi.org/10.1093/femsec/fiw194

Lundberg, D. S., Lebeis, S. L., Paredes, S. H., Yourstone, S., Gehring, J., Malfatti, S., … Dangl, J. L. (2012). Defining the core *Arabidopsis thaliana* root microbiome. *Nature*, *488*(7409), 86–90. https://doi.org/10.1038/nature11237

Mahoney, A. K., Yin, C., & Hulbert, S. H. (2017). Community structure, species variation, and potential functions of Rhizosphere-associated bacteria of different winter wheat. *Frontiers in Plant Science*, *8*, 132. https://doi.org/10.3389/fpls.2017.00132

Miller, G. L. (1959). Use of dinitrosalicylic acid reagent for determination of reducing sugar. *Analytical Chemistry*, *31*(3), 426–428. https://doi.org/10.1021/ac60147a030

Miotto-Vilanova, L., Jacquard, C., Courteaux, B., Wortham, L., Michel, J., Clément, C., … Sanchez, L. (2016). Burkholderia phytofirmans PsJN confers grapevine resistance against *Botrytis cinerea* via a direct antimicrobial effect combined with a better resource mobilization. *Frontiers in Plant Science*, *7*, 1236. https://doi.org/10.3389/fpls.2016.01236

Moin, M., Bakshi, A., Saha, A., Dutta, M., Madhav, S. M., & Kirti, P. B. (2016). Rice ribosomal protein large subunit genes and their spatio-temporal and stress regulation. *Frontiers in Plant Science*, *7*, 1284. https://doi.org/10.3389/fpls.2016.01284

Müller, D. B., Vogel, C., Bai, Y., & Vorholt, J. A. (2016). The plant microbiota: Systems-level insights and perspectives. *Annual Review of Genetics*, *50*, 211–234. https://doi.org/10.1146/annurev-genet-120215-034952

Naylor, D., DeGraaf, S., Purdom, E., & Coleman-Derr, D. (2017). Drought and host selection influence bacterial community dynamics in the grass root microbiome. *The ISME Journal*, *11*(12), 2691–2704. https://doi.org/10.1038/ismej.2017.118

Norris, M. H., Kang, Y., Wilcox, B., & Hoang, T. T. (2010). Stable, site-specific fluorescent tagging constructs optimized for *Burkholderia* species. *Applied and Environmental Microbiology*, *76*(22), 7635–7640. https://doi.org/10.1128/AEM.01188-10

Pagé, A. P., Tremblay, J., Masson, L., & Greer, C. W. (2019). Nitrogen- and phosphorus-starved *Triticum aestivum* show distinct belowground microbiome profiles. *PLoS One*, *14*(2), e0210538. https://doi.org/10.1371/journal.pone.0210538

Park, S. C., Lee, J. R., Shin, S. O., Park, Y., Lee, S. Y., & Hahm, K. S. (2007). Characterization of a heat-stable protein with antimicrobial activity from *Arabidopsis thaliana*. *Biochemical and Biophysical Research Communications*, *362*(3), 562–567. https://doi.org/10.1016/j.bbrc.2007.07.188

Pérez-de-Luque, A., Tille, S., Johnson, I., Pascual-Pardo, D., Ton, J., & Cameron, D. D. (2017). The interactive effects of arbuscular mycorrhiza and plant growth-promoting rhizobacteria synergistically enhance host plant defences against pathogens. *Scientific Reports*, *7*(1), 16409. https://doi.org/10.1038/s41598-017-16697-4

Pieterse, C. M., Zamioudis, C., Berendsen, R. L., Weller, D. M., Van Wees, S. C., & Bakker, P. A. (2014). Induced systemic resistance by beneficial microbes. *Annual Review of Phytopathology*, *52*, 347–375. https://doi.org/10.1146/annurev-phyto-082712-102340

Pieterse, C. M. J., van Wees, S. C. M., van Pelt, J. A., Knoester, M., Laan, R., Gerrits, H., … van Loon, L. C. (1998). A novel signaling pathway controlling induced systemic resistance in *Arabidopsis*. *The Plant Cell*, *10*(9), 1571–1580. https://doi.org/10.1105/tpc.10.9.1571

Ray, S. K., Macoy, D. M., Kim, W. Y., Lee, S. Y., & Kim, M. G. (2019). Role of RIN4 in regulating PAMP-triggered immunity and effector-triggered immunity: Current status and future perspectives. *Molecules and Cells*, *42*(7), 503–511. https://doi.org/10.14348/molcells.2019.2433

Rosier, A., Bishnoi, U., Lakshmanan, V., Sherrier, D. J., & Bais, H. P. (2016). A perspective on inter-kingdom signaling in plant-beneficial microbe interactions. *Plant Molecular Biology*, *90*(6), 537–548. https://doi.org/10.1007/s11103-016-0433-3

Rutowicz, K., Puzio, M., Halibart-Puzio, J., Lirski, M., Kotliński, M., Kroteń, M. A., … Jerzmanowski, A. (2015). A specialized histone H1 variant is required for adaptive responses to complex abiotic stress and related DNA methylation in *Arabidopsis*. *Plant Physiology*, *169*(3), 2080–2101. https://doi.org/10.1104/pp.15.00493

Saad, M. M., Eida, A. A., & Hirt, H. (2020). Tailoring plant-associated microbial inoculants in agriculture: A roadmap for successful application. *Journal of Experimental Botany*, *71*(13), 3878–3901. https://doi.org/10.1093/jxb/eraa111

Schaller, A., & Stintzi, A. (2009). Enzymes in jasmonate biosynthesis—Structure, function, regulation. *Phytochemistry*, *70*(13–14), 1532–1538. https://doi.org/10.1016/j.phytochem.2009.07.032

Schlaeppi, K., & Bulgarelli, D. (2015). The plant microbiome at work. *Molecular Plant-Microbe Interactions*, *28*(3), 212–217. https://doi.org/10.1094/MPMI-10-14-0334-FI

Setién, I., Fuertes-Mendizabal, T., González, A., Aparicio-Tejo, P. M., González-Murua, C., González-Moro, M. B., & Estavillo, J. M. (2013). High irradiance improves ammonium tolerance in wheat plants by increasing N assimilation. *Journal of Plant Physiology*, *170*(8), 758–771. https://doi.org/10.1016/j.jplph.2012.12.015

Shi, H., Shen, Q., Qi, Y., Yan, H., Nie, H., Chen, Y., … Tang, D. (2013). BR-SIGNALING KINASE1 physically associates with FLAGELLIN SENSING2 and regulates plant innate immunity in *Arabidopsis*. *Plant Cell*, *25*(3), 1143–1157. https://doi.org/10.1105/tpc.112.107904

Shi, H., Wang, B., Yang, P., Li, Y., & Miao, F. (2016). Differences in sugar accumulation and mobilization between sequential and non-sequential senescence wheat cultivars under natural and drought conditions. *PLoS One*, *11*(11), e0166155. https://doi.org/10.1371/journal.pone.0166155

Simonin, M., Dasilva, C., Terzi, V., Ngonkeu, E. L. M., Diouf, D., Kane, A., … Moulin, L. (2020). Influence of plant genotype and soil on the wheat rhizosphere microbiome: Evidences for a core microbiome across eight African and European soils. *FEMS Microbiology Ecology*, *96*(6). https://doi.org/10.1093/femsec/fiaa067

Singh, R., & Jwa, N. S. (2013). The rice MAPKK-MAPK interactome: The biological significance of MAPK components in hormone signal transduction. *Plant Cell Reports*, *32*(6), 923–931. https://doi.org/10.1007/s00299-013-1437-y

Spaepen, S., Bossuyt, S., Engelen, K., Marchal, K., & Vanderleyden, J. (2014). Phenotypical and molecular responses of *Arabidopsis thaliana* roots as a result of inoculation with the auxin-producing bacterium *Azospirillum brasilense*. *The New Phytologist*, *201*(3), 850–861. https://doi.org/10.1111/nph.12590

Thiergart, T., Zgadzaj, R., Bozsóki, Z., Garrido-Oter, R., Radutoiu, S., & Schulze-Lefert, P. (2019). Symbiosis genes impact microbial interactions between symbionts and multikingdom commensal communities. *MBio*, *10*(5).), https://doi.org/10.1128/mBio.01833-19

Torres, M. A., Dangl, J. L., & Jones, J. D. G. (2002). *Arabidopsis* gp91^{phox} homologues *AtrbohD* and *AtrbohF* are required for accumulation of reactive oxygen intermediates in the plant defense response. *Proceedings of the National Academy of Sciences*, *99*(1), 517. https://doi.org/10.1073/pnas.012452499

Tortora, M. L., Díaz-Ricci, J. C., & Pedraza, R. O. (2012). Protection of strawberry plants (*Fragaria ananassa* Duch.) against anthracnose disease induced by *Azospirillum brasilense*. *Plant and Soil*, *356*(1), 279–290. https://doi.org/10.1007/s11104-011-0916-6

Trouvelot, A., Kough, J. L., & Gianinazzi-Pearson, V. (1986). Mesure du taux de mycorhization VA d'un systeme radiculaire. Recherche de methods d'estimation ayant une signification fonctionnelle. In S. Gianinazzi (Ed.), *Physiological and genetical aspects of Mycorrhizae* (pp. 217–221). Paris, France: INRA.

Tsolakidou, M. D., Stringlis, I. A., Fanega-Sleziak, N., Papageorgiou, S., Tsalakou, A., & Pantelides, I. S. (2019). Rhizosphere-enriched microbes as a pool to design synthetic communities for reproducible beneficial outputs. *FEMS Microbiology Ecology*, *95*(10). https://doi.org/10.1093/femsec/fiz138

Uroz, S., Courty, P. E., & Oger, P. (2019). Plant symbionts are engineers of the plant-associated microbiome. *Trends in Plant Science*, *24*(10), 905–916. https://doi.org/10.1016/j.tplants.2019.06.008

Van der Heijden, M. G. A., Klironomos, J. N., Ursic, M., Moutoglis, P., Streitwolf-Engel, R., Boller, T., … Sanders, I. R. (1998). Mycorrhizal fungal diversity determines plant biodiversity, ecosystem variability and productivity. *Nature*, *396*(6706), 69–72. https://doi.org/10.1038/23932

Vannini, C., Marsoni, M., Scoccianti, V., Ceccarini, C., Domingo, G., Bracale, M., & Crinelli, R. (2019). Proteasome-mediated remodeling of the proteome and phosphoproteome during kiwifruit pollen germination. *Journal of Proteomics*, *192*, 334–345. https://doi.org/10.1016/j.jprot.2018.09.014

Verdier, V., Triplett, L. R., Hummel, A. W., Corral, R., Cernadas, R. A., Schmidt, C. L., … Leach, J. E. (2012). Transcription activator-like (TAL) effectors targeting OsSWEET genes enhance virulence on diverse rice (*Oryza sativa*) varieties when expressed individually in a TAL effector-deficient strain of *Xanthomonas oryzae*. *New Phytologist*, *196*(4), 1197–1207. https://doi.org/10.1111/j.1469-8137.2012.04367.x

Vorholt, J. A., Vogel, C., Carlström, C. I., & Müller, D. B. (2017). Establishing causality: Opportunities of synthetic communities for plant microbiome research. *Cell Host & Microbe*, *22*(2), 142–155. https://doi.org/10.1016/j.chom.2017.07.004

Wang, C., Zien, C. A., Afitlhile, M., Welti, R., Hildebrand, D. F., & Wang, X. (2000). Involvement of phospholipase D in wound-induced accumulation of jasmonic acid in *Arabidopsis*. *Plant Cell*, *12*(11), 2237–2246. https://doi.org/10.1105/tpc.12.11.2237

Wang, S., Zhang, Y., Song, Q., Fang, Z., Chen, Z., Zhang, L., … Zhang, G. (2017). Mitochondrial dysfunction causes oxidative stress and tapetal apoptosis in chemical hybridization reagent-induced male sterility in wheat. *Frontiers in Plant Science*, *8*, 2217. https://doi.org/10.3389/fpls.2017.02217

Wasternack, C., & Hause, B. (2013). Jasmonates: Biosynthesis, perception, signal transduction and action in plant stress response, growth and development. An update to the 2007 review in Annals of Botany. *Annals of Botany*, *111*(6), 1021–1058. https://doi.org/10.1093/aob/mct067

Wisniewski-Dyé, F., Borziak, K., Khalsa-Moyers, G., Alexandre, G., Sukharnikov, L. O., Wuichet, K., … Zhulin, I. B. (2011). *Azospirillum* genomes reveal transition of bacteria from aquatic to terrestrial environments. *PLoS Genetics*, *7*(12), e1002430–e1002430. https://doi.org/10.1371/journal.pgen.1002430

Wu, X., Xiong, E., Wang, W., Scali, M., & Cresti, M. (2014). Universal sample preparation method integrating trichloroacetic acid/acetone precipitation with phenol extraction for crop proteomic analysis. *Nature Protocols*, *9*(2), 362–374. https://doi.org/10.1038/nprot.2014.022

Yasuda, M., Isawa, T., Shinozaki, S., Minamisawa, K., & Nakashita, H. (2009). Effects of colonization of a bacterial endophyte, *Azospirillum* sp. B510, on disease resistance in rice. *Bioscience, Biotechnology, and Biochemistry*, *73*(12), 2595–2599. https://doi.org/10.1271/bbb.90402

Zeffa, D. M., Perini, L. J., Silva, M. B., de Sousa, N. V., Scapim, C. A., Oliveira, A. L. M., … Azeredo Gonçalves, L. S. (2019). *Azospirillum brasilense* promotes increases in growth and nitrogen use efficiency of maize genotypes. *PLoS One*, *14*(4), e0215332. https://doi.org/10.1371/journal.pone.0215332

Zhao, J., Zhou, H., Zhang, M., Gao, Y., Li, L., Li, M., … Li, X. (2016). Ubiquitin-specific protease 24 negatively regulates abscisic acid signalling in *Arabidopsis thaliana*. *Plant, Cell & Environment*, *39*(2), 427–440. https://doi.org/10.1111/pce.12628

SUPPORTING INFORMATION

Additional supporting information may be found online in the Supporting Information section at the end of this article.

How to cite this article: Vannini C, Domingo G, Fiorilli V, et al. Proteomic analysis reveals how pairing of a Mycorrhizal fungus with plant growth-promoting bacteria modulates growth and defense in wheat. *Plant Cell Environ*. 2021;1–15. https://doi.org/10.1111/pce.14039